A novel closed-form aolution for the inverse kinematics of redundant manipulators through workspace analysis

Isiah Zaplana[a,*], Luis Basanez[a]

[a] *Institute of Industrial and Control Engineering, Technical University of Catalonia, 08028 Barcelona, Spain*

Abstract

This work addresses the inverse kinematic problem for redundant serial manipulators. Its importance relies on its effect in the programming and control of redundant robots. Besides, no general closed-form techniques have been developed so far. In this paper, redundant manipulators are reduced to non-redundant ones by selecting a set of joints, denoted *redundant joints*, and parametrizing its joint variables. This selection is made through a workspace analysis which also provides an upper bound for the number of different closed-form solutions for a given pose. Once these joints have been identified several closed-form methods developed for non-redundant manipulators can be applied for obtaining the analytical solutions. Finally, particular instances for the parametrized joints variables are determined depending on the task to be executed. Different criteria and optimization functions can be defined for that purpose.

Keywords: Inverse kinematics, robotics, redundant manipulators, workspace analysis

1. Introduction

A serial robot manipulator is an open kinematic chain made up of a sequence of rigid bodies, called links, connected by means of kinematic pairs, called joints, that provide relative motion between consecutive links. At the end of the last link, there is a tool or device, called end-effector.

From a kinematic point of view, the end-effector position and orientation (pose) of a manipulator can be expressed as a differentiable function $f : \mathcal{C} \rightarrow X$ that relates the space of joint variables, denoted configuration space $\mathcal{C}$, with the space of all positions and orientations of the end-effector with respect to a reference frame, known as the operational space X. For serial manipulators, a frame used to describe the relative position and orientation is attached to

*Corresponding author

Email addresses: isiah.zaplana@upc.edu (Isiah Zaplana), luis.basanez@upc.edu (Luis Basanez)

each joint of the manipulator. The relations between consecutive joint frames can be expressed by homogeneous matrices based in the D-H parameters [1, 2, 3, 4]. Therefore, each joint i has associated, together with the corresponding orthonormal frame $\{\boldsymbol{o}_i, \boldsymbol{x}_i, \boldsymbol{y}_i, \boldsymbol{z}_i\}$, a homogeneous matrix that relates this frame to the precedent one (the first joint frame is related to the world frame). The function f, known as the kinematic function, can be represented with these homogeneous matrices. Deriving the kinematic function f with respect to time, a relation in the rate domain is obtained:

$$\dot{\boldsymbol{x}} = J(\boldsymbol{q})\dot{\boldsymbol{q}} \tag{1}$$

where $\dot{\boldsymbol{x}}$ denotes the velocity vector of the end-effector; $\dot{\boldsymbol{q}}$, the vector of the joint velocities; and J, the Jacobian matrix associated to the manipulator. A manipulator is said to have *n degrees of freedom (DOF)* if its configuration can be minimally specified by n variables. For a serial manipulator, the number and nature of the joints determine the number of DOF. For the task of positioning and orientating its end-effector in the space, the manipulators with more than 6 DOF are called redundant while the rest are non-redundant. Redundant manipulators have $m = n - 6$ *degrees of redundancy*.

There are two types of Jacobian matrix: the geometric Jacobian $J_G(\boldsymbol{q})$ and the analytical Jacobian $J_A(\boldsymbol{q})$, depending if the last three components of $\dot{\boldsymbol{x}}$ in (1) represent the angular or the rotational velocity of the end effector, respectively. If J_i denotes the ith column of $J_G(\boldsymbol{q})$,

$$J_i = \begin{cases} \begin{bmatrix} \boldsymbol{z}_i \times (\boldsymbol{o}_n - \boldsymbol{o}_i) \\ \boldsymbol{z}_i \end{bmatrix} & \text{if } i \text{ is revolute} \\ \begin{bmatrix} \boldsymbol{z}_i \\ 0 \end{bmatrix} & \text{if } i \text{ is prismatic} \end{cases}$$

where $\times$ denotes the cross product of two vectors in $\mathbb{R}^3$.

One of the most important kinematic problems for serial manipulators is the inverse kinematic problem. This problem consists of obtaining the joint variables, i.e. the configuration, associated to a particular pose. This configuration may not be unique, since non-redundant manipulators have up to sixteen different configurations for the same particular pose [5], while for redundant manipulators this number is unbounded [3, 4]. The methods to solve the inverse kinematics problem for serial manipulators are categorized into two groups:

a) Analytical or closed-form methods: All the solutions are expressed as functions in terms of the pose.

b) Numerical methods: Starting with an initial configuration $\boldsymbol{q}_0$, an iterative process returns a good approximation $\widetilde{\boldsymbol{q}}$ of one of the solutions.

The *closed-form methods* strongly depend on the geometry of the manipulator and, therefore, are not general enough. However, they are computationally efficient and give all the solutions for a given pose. In his PhD thesis, Pieper

[5] develops a procedure for obtaining the closed-form solutions for a class of serial manipulators, i.e., the manipulators with three consecutive joints whose axes are either parallel or intersect at a single point (if these three consecutive joints are the last three, the robot is said to have *spherical wrist*). Later, Paul [6] establishes a more rigorous and generic method based on the handling of the homogeneous matrices that can be applied to manipulators of other kind. The main recent contributions include the use of Lagrange multipliers [7], the definition of imaginary links for redundant manipulators [8, 9], the definition of the arm angle parameter [10, 11, 12] and different geometric methods [13, 14, 15, 16].

On the other hand, *numerical methods* usually work with any manipulator, but they suffer from several drawbacks like high computational cost and execution time, existence of local minima and numerical errors. Moreover, only one of the sixteen (infinite) possible solutions is obtained for non-redundant (redundant) manipulators. The most extended numerical approaches are the Jacobian-based methods, in which the relation (1) is inverted and solved iteratively. Inverting the Jacobian matrix is not always possible. For redundant manipulators, $J(\boldsymbol{q})$ is not a square matrix while for non-redundant manipulators $\det(J(\boldsymbol{q}))$ vanishes at singularities [3, 4]. To handle with these situations, alternative methods are used like pseudoinverse, transpose, damped least-squares and local optimization [3, 17, 18, 19, 20, 21, 22, 23, 24, 25, 26, 27, 28]. Other numerical methods include the use of augmented Jacobian [29], conformal geometry algebra [30, 31], Crank-Nicholson methods [32] and reachability maps [33].

The importance of the inverse kinematic problem relies on its role in the programming and control of serial robots. Besides, this problem becomes of great significance for redundant manipulators because, existing an infinite number of solutions for a particular pose, manipulability measures can be defined for selecting a particular solution. Among all the methods presented in this section, closed-form ones are the most suitable for redundant manipulators as they allow to obtain the set of all solutions with a small computational cost. This paper proposes a novel method for deriving closed-form solutions for the inverse kinematics of redundant serial manipulators. These solutions are given as m-parameter famiies of functions depending on the end-effector' pose. Redundant manipulators are reduced into non-redundant ones by parametrization of a set of joint variables. These joints will be denoted as *redundant joints*. The selection of such joints is crucial and it is done using global rank deficiency conditions of the Jacobian matrix and workspace's volume analysis. An upper bound for the number of different m-parameter families of closed-form solutions is given. This number depends on the degrees of redundancy. Once the redundant joints are selected, the inverse kinematics of the non-redundant manipulator is solved analytically using either Pieper, Paul or other geometric methods. Finally, the particular values of the parametrized joint variables can be determined using manipulability measures or optimization criteria. The rest of the paper is organized as follows: Section 2 reviews the related work. In Section 3, the methodology is presented. This section is divided into three parts:

in Section 3.1 an upper bound for the number of different closed-form solutions associated to a particular pose is given; Section 3.2 displays the different criteria for the selection of redundant joints, while in Section 3.3 several closed-form methods are used for the non-redundant reduced manipulator. Examples of two different redundant manipulators are given in Section 4. Finally, Section 5 presents the conclusions.

2. Related Work

First mentions of redundant joints are found in [34, 35, 36]. In these papers a redundant manipulator is designed from a known non-redundant one. In this context, the authors assume that the added joint is the redundant one. Later, in [37] several closed-form solutions for an anthropomorphic manipulator are derived by fixing the different joint variables at an arbitrary value. Following that idea, in [38, 39] the authors develop a criterion for discarding some of these joints as redundant ones. This criterion is based on a geometric characterization proposed by Heiss [40]. Heiss defines a class of 6 DOF manipulators, called *globally degenerated manipulators*, that have limited its motion in the whole workspace, i.e., they cannot translate or rotate its end-effector through an axis for any given configuration. In [38, 39] the characterization given by Heiss is resumed in the following theorem:

Theorem 2.1. *A serial manipulator of 6 DOF is globally degenerated if, and only if,* $\det(J_G(\boldsymbol{q})) = 0$ *for all* $\boldsymbol{q} \in \mathcal{C}$.

The criterion proposed in [38] consist on discarding as redundant those joints that, once their joint variables are fixed at some value, leave a globally degenerated non-redundant manipulator. Applied to anthropomorphic manipulators, it is shown that just the fourth joint should be discarded as an option for being the redundant joint. Then, the idea collected in [37] is applied for obtaining different closed-form solutions for the anthropomorphic manipulator. The main drawback of these approaches relies on the number of closed-form solutions obtained for each pose. While in [37] four one-parameter families of solutions are developed for a 7 DOF anthropomorphic manipulator, in [38] up to six one-parameter families of solutions are developed for the same manipulator. The use of either of the closed-form solutions depends on the task executed. If, instead of considering a 7 DOF redundant manipulator, a 8 DOF robot is considered there will be up to $C(8, 2) = 28$ 2-parameter families of solutions. In general, for an n DOF redundant manipulator there will be up to $C(n, n-6)$ $(n-6)$-parameter families of solutions. This large set of solutions increases the difficulties for selecting one of them for each particular pose.

On the other hand, in [41] a selection of redundant joints based on the null space range of each joint is proposed, while in [42] the authors base their selection on the null space of the Jacobian matrix. These approaches turn to be impractical due to their computational cost. Besides, their implementation become extremely difficult for more than one degree of redundancy. The approaches collected in [22, 43, 44, 45, 46] are focused on developing strong and

general closed-form methods for non-redundant manipulators. In these works redundant joints are selected arbitrarily. Finally, [10, 11, 12, 47] are recent examples of the arm angle parameter use. This parameter, usually denoted by φ, is defined for anthropomorphic manipulators attending to the relation between shoulder (three first joints), elbow (fourth joint) and wrist (three last joints). Therefore, φ can be regarded as a joint variable, and thus, it can be considered as defining the redundant joint.

The approach given in [38, 39] is the most interesting and easy to implement. However, as it has been shown above, this approach is not easily generalized for n DOF redundant manipulators. Besides, it does not represent a method for selecting redundant joints but to discard some of them as candidates. The procedure proposed in the present paper includes such criterion but also uses a workspace's analysis to prove that it is enough with a maximum of 2^m m-parameter families of closed-form solutions. This number is always much smaller than $C(n, n-6)$. Besides, a criterion for selecting, given a particular pose, one of these 2^m closed-form solutions is provided.

Many authors have dealt with the problem of representing effectively the serial manipulators workspace: in [48] an strategy for the identification of the workspace area of planar serial manipulators is developed, while in [49, 50, 51] an iterative process that only works for serial manipulators with revolute joints is defined. This method attains the analytical equations of the workspace defining the end-effector as a three dimensional point that is rotated from the n-th joint to the first one. Then, a cross section is obtained by taking $q_1 = 0$. On the other hand, in [52, 53] the authors define the interior and exterior boundaries of serial manipulators workspace using the singular surfaces achieved from the Jacobian matrix. Then, the total volume of the workspace is calculated using the Divergence Theorem.

Next section focuses on how to exploit the shape and quantitative properties, such as area and volume, of serial manipulators workspace and how these properties can be used in the identification of redundant joints.

3. Closed-form Solutions through Workspace Analysis

3.1. Closed-form Solutions Upper Bound

As it has been mentioned in the preceding section, some authors develop up to four or six families of solutions for a 7 DOF manipulator. In this section an upper bound for the number of different closed-form solutions for a particular pose is given. It will be proven that is enough with a maximum of 2^m m-parameter families of solutions for a n DOF manipulator.

For simplicity, the following notation will be used:

- $\mathcal{R}$ denotes a serial manipulator of n DOF.
- p denotes the number of prismatic joints of $\mathcal{R}$.
- $\mathcal{W}$ denotes the workspace of $\mathcal{R}$, generated by its revolute joints.

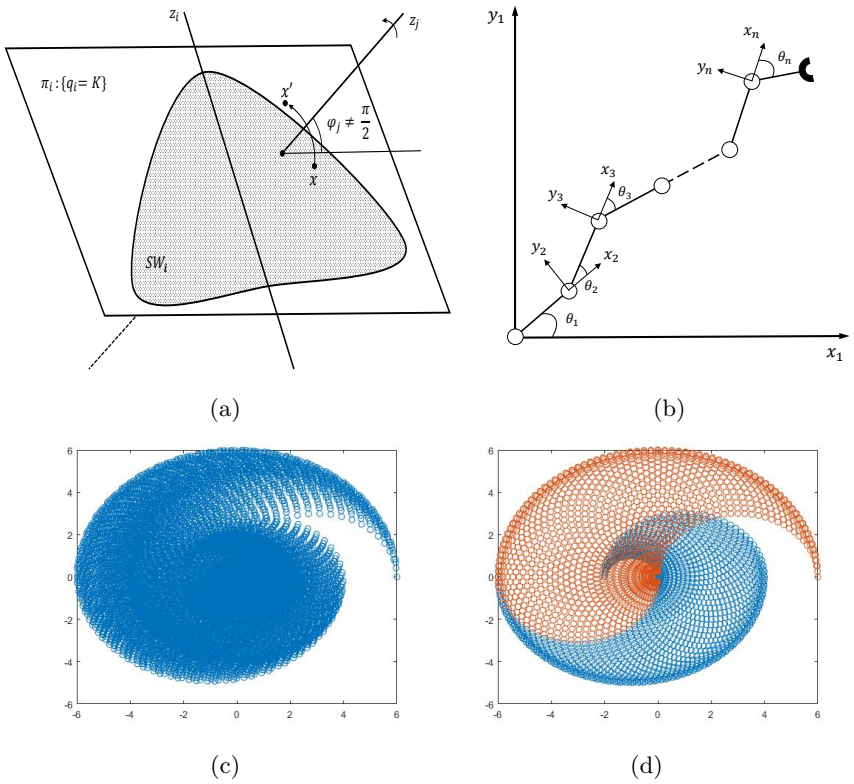

Figure 1: (a) Cross section $\mathcal{SW}_i$ of $\mathcal{W}$ for a given value of q_i where an arbitrary point $\boldsymbol{x} \in \mathcal{SW}_i$ under the action of $\boldsymbol{z}_j$ is transformed into $\boldsymbol{x}' \notin \mathcal{SW}_i$; (b) Schematic representation of a planar manipulator; (c) Workspace of the three-link manipulator and (d) Workspaces regions after fixing the first and the second joints respectively

- $\mathcal{W}_i$ denotes the volume of $\mathcal{W}$ once the joint i is fixed at some value.

The idea is to prove that, given $\mathcal{W}$, one of the two following statement holds:

$$\text{There exists } 2 \leq i \leq n \text{ such that } \mathcal{W}_i = \mathcal{W} \tag{2}$$

$$\text{There exist } 2 \leq j \neq k \leq n \text{ such that } \mathcal{W}_j \cup \mathcal{W}_k = \mathcal{W} \tag{3}$$

For $n = 7$ (or, equivalently, $m = 1$), if statement (2) holds, as $\mathcal{W}_i$ is obtained when the joint i is fixed, the redundant manipulator $\mathcal{R}$ has been reduced into a non-redundant one. The closed-form solutions for the inverse kinematics will form a single one-parameter family of solutions depending on q_i. However, if statement (3) holds, there will be two different non-redundant reduced manipulators. Therefore, two different one-parameter families of solutions will be obtained (one depending on q_j and the other on q_k).

If, conversely, $n > 7$ (or, equivalently $m > 1$) the process is repeated with $\mathcal{W}_i$ or with $\mathcal{W}_j, \mathcal{W}_k$. The reasoning is exactly the same, since $\mathcal{W}_i, \mathcal{W}_j$ and $\mathcal{W}_k$

can be seen as the workspace of a manipulator of $n-1$ DOF. The maximum number of subregions of the original workspace that can be obtained for each degree of redundancy is two. So, given the recursiveness of the procedure, the maximum number of subregions will be 2^m. As each one generates a family of solutions, there will be up to 2^m m-parameter families of closed-form solutions. By the same reason, the minimum number of m-parameter families of solutions will be one. Therefore, for any given manipulator $\mathcal{R}$ with n DOF and m degrees of redundancy the number r of different solution families verifies:

$$1 \leq r \leq 2^m.$$

It only remains to prove that, for any redundant manipulator $\mathcal{R}$, either statement (2) or statement (3) holds.

First of all, since the effect of the prismatic joints in the workspace of $\mathcal{R}$ is just the translation of the volume generated by the following joints and since, given a pose, it is easy to obtain the values of the prismatic joint variables, i.e., the solution of the inverse kinematics for these joints, their joint variables can be fixed at particular instances for allowing the study of $\mathcal{W}$.

Let denote by $\mathcal{R}_{j_1}, \mathcal{R}_{j_2}, \ldots, \mathcal{R}_{j_p}$ the prismatic joints of $\mathcal{R}$. Then, each of their joint variables $d_{j_1}, d_{j_2}, \ldots, d_{j_p}$ moves within $[d_{j_i\text{Low}}, d_{j_i\text{Up}}]$. As $\mathcal{W}$ is generated only by the revolute joints of $\mathcal{R}$, each d_{j_i} can be fixed at a particular value, selected, for instance, to make $\mathcal{W}$ as compact as possible. Although the values of the prismatic joint variables are, in general, positive, depending on where the world frame is placed, different cases can arise. Such cases are treated as follows:

- $0 \in [d_{j_i\text{Low}}, d_{j_i\text{Up}}] \Longrightarrow d_{j_i} = 0.$
- $[d_{j_i\text{Low}}, d_{j_i\text{Up}}] \subset \mathbb{R}^+ \setminus \{0\} \Longrightarrow d_{j_i} = d_{j_i\text{Low}}.$
- $[d_{j_i\text{Low}}, d_{j_i\text{Up}}] \subset \mathbb{R}^- \setminus \{0\} \Longrightarrow d_{j_i} = d_{j_i\text{Up}}.$

As only the revolute joints of $\mathcal{R}$ are going to be considered, let $\boldsymbol{z}_i$ be the first revolute joint of $\mathcal{R}$. Then, $\mathcal{W}$ is of revolution around $\boldsymbol{z}_i$ and, as a result, the study of $\mathcal{W}$ can be performed over a $\boldsymbol{x}_i$-$\boldsymbol{z}_i$ cross section of it. For a redundant manipulator, such cross section is obtained by fixing q_i at a particular value. Besides, it is also necessary to fix other joints like, in particular, all the rotational joints whose axes are not orthogonal to $\boldsymbol{z}_i$. To prove this remark let suppose that there exists $\boldsymbol{z}_j$ such that $\boldsymbol{z}_j$ and $\boldsymbol{z}_i$ are not mutually orthogonal. If $\boldsymbol{z}_j$ is not fixed, then its rotational action generates a volume that escapes from the section obtained by setting $q_i = k$ (figure 1a). Thus, the cross section area is generated by the joints whose axes are orthogonal to $\boldsymbol{z}_i$ while the rest are fixed at particular values. Let s denote the number of joints whose axes are orthogonal to $\boldsymbol{z}_i$. Different cases should be treated:

$\boxed{s = \{0, 1, 2\}}$

There are no joint axes, one joint axis or two joint axes orthogonal to $\boldsymbol{z}_i$. Since

$\mathcal{R}$ is redundant, at least there are three, two or one more joints whose variables are fixed - as they are not orthogonal to $\boldsymbol{z}_i$. Two different situations arise: one of the other joint axes is contained in the cross section plane or intersects it. Both cases are treated analogously. Let denote by $\mathcal{SW}$ the cross section area obtained by setting $q_i = k$. As it has been commented before and since $s < 3$, this cross section is generated by fixing also the joints whose axes are not orthogonal to $\boldsymbol{z}_i$. Let suppose that there is at least one joint whose axis, $\boldsymbol{z}_j$, either is contained in $\mathcal{SW}$ or intersects $\mathcal{SW}$ (not orthogonally). Then, $\mathcal{SW} \subset \mathcal{W}_j$. Moreover, if the same cross section is taken from $\mathcal{W}_j$, $\mathcal{SW}_j$, then

$$\mathcal{SW}_j = \mathcal{SW} \tag{4}$$

As $\mathcal{W}$ is of revolution around $\boldsymbol{z}_i$, rotating q_i turns (4) into $\mathcal{W}_j = \mathcal{W}$ which gives the desirable result.

$\boxed{s \geq 3}$

From $s = 3$, induction over s can be used for completing the proof. Again, two different situations can arise:

- There exists a joint whose axis, $\boldsymbol{z}_k$, is contained in the cross section obtained by setting $q_i = k$ or intersects it (not orthogonally).
- The only revolute joints contributing to position the end-effector are i and the s joints whose axes are orthogonal to $\boldsymbol{z}_i$.

For the first situation, the previous reasoning can be used to prove that $\mathcal{W}_k = \mathcal{W}$. For the second, it is clear that $\mathcal{SW}$ is generated by the s joints whose axes are orthogonal to $\boldsymbol{z}_i$ (and, as a result, normal to $\mathcal{SW}$). In particular, if $i_1, \ldots, i_s$ denote these joints and $\mathcal{SW}_{i_j}$ denote the plane section of $\mathcal{SW}$ obtained when the joint i_j is fixed, then

$$\mathcal{SW}_{i_1} \cup \mathcal{SW}_{i_2} \cup \cdots \cup \mathcal{SW}_{i_s} = \mathcal{SW} \tag{5}$$

It is sufficient with proving that:

$$\exists i_j, i_k \quad : \quad \mathcal{SW}_{i_j} \cup \mathcal{SW}_{i_k} = \mathcal{SW} \tag{6}$$

If so, rotating q_i gives that

$$\mathcal{W}_j \cup \mathcal{W}_k = \mathcal{W},$$

which would complete the proof.

To prove it, let notice that $\mathcal{SW}$ can be seen as the workspace of a s-link planar manipulator (figure 1b). Thus, (6) is equivalent to prove that the workspace of a s-link planar manipulator can be split in two subregions associated with two fixed joints. This proof will be performed using induction over s.

For $s = 3$, a 3-link planar manipulator is obtained. Figure 1c depicts the workspace of an example of a manipulator of this kind. In general, the end

effector position vector of a 3-link planar manipulator is:

$$\boldsymbol{p} = \begin{pmatrix} a_1c_1 + a_2c_{12} + a_3c_{123} \\ a_1s_1 + a_2s_{12} + a_3s_{123} \\ 0 \end{pmatrix},$$

where a_i is the length of link i and $c_1 = \cos(q_{i_1}), s_1 = \sin(q_{i_1}), c_{12} = \cos(q_{i_1} + q_{i_2}), s_{12} = \sin(q_{i_1} + q_{i_2}), c_{123} = \cos(q_{i_1} + q_{i_2} + q_{i_3})$ and $s_{123} = \sin(q_{i_1} + q_{i_2} + q_{i_3})$. Figure 1d shows that it is enough with taking $\mathcal{SW}_{i_1}, \mathcal{SW}_{i_2}$ for obtaining $\mathcal{SW}$. To prove that this is a general result let suppose, by contradiction, that

$$\mathcal{SW}_{i_1} \cup \mathcal{SW}_{i_2} \neq \mathcal{SW}$$

for all the constant values $q_{i_1} = k_1$ and $q_{i_2} = k_2$ of joints i_1 and i_2. Then, there exists $x \in \mathcal{SW}$ such that $x \notin \mathcal{SW}_{i_1}$ and $x \notin \mathcal{SW}_{i_2}$ for all $q_{i_1} = k_1$ and $q_{i_2} = k_2$. Now, by (5) $x \in \mathcal{SW}_{i_3}$ for some constant value $q_{i_3} = k_3$. Since the position vector for the 3-link planar manipulator depends on q_{i_1}, q_{i_2} and q_{i_3}, if q_{i_1} (or q_{i_2}) is considered as a parameter, i.e., its value varies in its range, then q_{i_2} (or q_{i_1}) has a particular value for x. Then, $x \in \mathcal{SW}_{i_2}$ (or $x \in \mathcal{SW}_{i_1}$), which is a contradiction.

Now, let suppose that the statement holds for s. As in the case of $s = 3$ it is enough to prove that

$$\mathcal{SW}_{i_1}(s+1) \cup \mathcal{SW}_{i_2}(s+1) = \mathcal{SW}(s+1)$$

where the notation $(s+1)$ highlights that the sections belong to the $(s+1)$-link manipulator. Let suppose, again by contradiction, that

$$\mathcal{SW}_{i_1}(s+1) \cup \mathcal{SW}_{i_2}(s+1) \neq \mathcal{SW}(s+1)$$

for all the constant values $q_{i_1} = k_1$ and $q_{i_2} = k_2$. Then, there exists $x \in \mathcal{SW}(s+1)$ such that $x \notin \mathcal{SW}_{i_1}(s+1)$ and $x \notin \mathcal{SW}_{i_2}(s+1)$ for all $q_{i_1} = k_1$ and $q_{i_2} = k_2$. Now, again by (5), $x \in \mathcal{SW}_{i_\ell}(s+1)$ for some $3 \leq \ell \leq s+1$ and some constant value $q_{i_\ell} = k_\ell$. Since $\mathcal{SW}_{i_\ell}(s+1)$ can be seen as the workspace of a s-link planar manipulator, the hypothesis of induction implies that $x \in \mathcal{SW}_{i_1}(s)$ or $x \in \mathcal{SW}_{i_2}(s)$ for some constant values $q_{i_1} = k_1$ and $q_{i_2} = k_2$. But now, it is clear that, for the same constant values k_1, k_2:

$$\mathcal{SW}_{i_1}(s) \subset \mathcal{SW}_{i_1}(s+1)$$
$$\mathcal{SW}_{i_2}(s) \subset \mathcal{SW}_{i_2}(s+1)$$

These relations are true for every extension of a s-link planar manipulator to a $(s+1)$-link planar manipulator. In particular, they are true if the extension of the s-link planar manipulator is made to obtain the $(s+1)$-link planar manipulator of the beginning of this part of the proof. Then, $x \in \mathcal{SW}_{i_1}(s+1)$ or $x \in \mathcal{SW}_{i_2}(s+1)$ for the constant values $q_{i_1} = k_1$ and $q_{i_2} = k_2$. This gives the desirable contradiction.

Given that there could be many other joints fixed at some value, this result is not useful for the identification of the redundant joints but to prove the upper bound in the number of different families of closed-form solutions. Next section displays the criteria for efficiently selecting the redundant joints.

Algorithm 1 Globally Degeneracy Criterion

Require: $6 \times n$ Jacobian matrix J
Ensure: Integers $i_1, \ldots, i_m$

```
procedure GLOBALLY DEGENERACY TEST
    for 1 ≤ i ≤ n do
        M ← J[1:6; 1:(i−1), (i+1):n]
        if M square then
            det ← det(M)
            if det == 0 then
                return i
            else go to step 2
        else Globally Degeneracy Test← M
```

3.2. Identification of Redundant Joints

Once it has been proven that there is a maximum of 2^m closed-form families of solutions, the criteria for the identification of which joints are the redundant ones are presented. These criteria are based on the global rank deficiency of the Jacobian matrix and on a workspace analysis.

If $\mathcal{R}_1, \ldots, \mathcal{R}_n$ denote the joints of a redundant manipulator $\mathcal{R}$ with n DOF, then not every $\mathcal{R}_i$ is candidate for being the redundant joint. First, a list of discarding conditions is shown. If $\mathcal{R}_i$ meets any condition of the list it will be discarded as candidate. The workspace analysis is performed over the remaining joints.

Discarding List 3.1.

- $\mathcal{R}_i$ *is a prismatic joint.*
- $\mathcal{R}_i$ *is one of the three joints that conforms a spherical wrist.*
- $\mathcal{R}_i$*, if it is fixed at some value, leaves a globally degenerated manipulator.*

Theorem 2.1 provides a simple and easy to implement way of testing the third condition of 3.1. Algorithm 1 returns, given the Jacobian matrix of a manipulator $\mathcal{R}$, the joints $\mathcal{R}_{i_1}, \ldots, \mathcal{R}_{i_m}$ that leave a globally degenerated subchain.

Once the joints meeting any condition of 3.1 are discarded, a workspace analysis is performed over the remaining joints in order to choose the redundant ones. For the sake of simplicity, the analysis is described in detail for the case of one degree of redundancy. After that, it is generalized. This analysis consists of two main steps:

I As explained before, the prismatic joint variables are fixed - they cannot be the redundant joints and their effect in $\mathcal{W}$ is just the translation of the volume generated by the following joints. Once $d_{j_1}, d_{j_2}, \ldots, d_{j_p}$ have been fixed, the manipulator is made up of revolute joints. Now, Algorithm 2 generates the swept volume of $\mathcal{W}$ and $\mathcal{W}_1, \ldots, \mathcal{W}_m$. As it has been shown

Algorithm 2 3D Workspace Generation

Require: D-H parameters DH, Forward Kinematics function FK
Ensure: Workspaces $\mathcal{W}, \mathcal{W}_1, \ldots, \mathcal{W}_m$

procedure WORKSPACE GENERATION
  cont$\leftarrow 0$
  for $1 \leq i \leq$ #DOF **do**
    if joint i is revolute **then**
      $\Delta_i \leftarrow$ discretization q_i
      cont $\leftarrow$ cont+1
      if joint i does not meet 3.1 **then**
        I $\leftarrow i$
    else $d_i \leftarrow 0$
  T $\leftarrow$FK(DH)
  P $\leftarrow$ Position vector(T)
  $\mathcal{W} \leftarrow \mathrm{P}(\Delta_1, \ldots, \Delta_{\mathrm{cont}})$
  for $i \in I$ **do**
    $q_i \leftarrow 0$
    $\mathrm{T}_i \leftarrow$FK(DH)
    $\mathrm{P}_i \leftarrow$ Position vector(T_i)
    $\mathcal{W}_i \leftarrow \mathrm{P}(\Delta_1, \ldots, \Delta_{i-1}, \Delta_{i+1}, \ldots, \Delta_{\mathrm{cont}})$

in the precedent section, either there exists i such that $\mathcal{W}_i = \mathcal{W}$ or there exist $i \neq j$ such that $\mathcal{W}_i \cup \mathcal{W}_j = \mathcal{W}$. Direct visualization allows to deduce which one of these situations happen for every redundant manipulator $\mathcal{R}$. If it seems that the two situations hold with different joints, then only the case $\mathcal{W}_i = \mathcal{W}$ will be considered since it is simpler and leads to a single family of solutions.

II To confirm what it has been observed through direct visualization, the ***x*-*z*** cross section of $\mathcal{W}$ is compared with the cross sections of either $\mathcal{W}_i$ or $\mathcal{W}_i$ and $\mathcal{W}_j$. As $\mathcal{W}$ is of revolution around its first revolute joint, the ***x*-*z*** cross section can be obtained by setting $q = 0$ where q is the first revolute joint variable of $\mathcal{R}$. This cross section can be obtained through a discretization of the joint variables that generate it. Apart from comparing the cross sections, a quantitative analysis based on the area can be performed. As $\mathcal{R}$ is made up of revolute joints the cross sections are composed of circle sectors. Therefore, for a given cross section the area can be obtained analytically using the expression:

$$A = \sum_i \pi r_i^2 \frac{\alpha_i}{360^\circ} \tag{7}$$

where r_i denotes the radius of each circle sector and α_i denotes its angle. For some geometric structures it could be difficult to find out the radius or angle of a particular circle sector. For those cases, given a discretization

of the cross section, the following numerical expression for the area can be used [50]:

$$A = \sum_{x_{\min}}^{x_{\max}} (z_{\max}(x) - z_{\min}(x))\Delta_x \tag{8}$$

where $x_{\min}$ and $x_{\max}$ denote the extreme values of the cross section abscissa while $z_{\min}$ and $z_{\max}$ denote the extreme values of the ordinate. However, (8) works only for convex cross sections without voids. Otherwise, (8) changes into the following one:

$$A = \sum_{x_{\min}}^{x_{\max}} (z_{\max}(x) - z_{1\max}(x) - \cdots + z_{\mathrm{L}\max}(x) - z_{\min}(x))\Delta_x \tag{9}$$

where $z_{1\max}(x), \ldots, z_{\mathrm{L}\max}(x)$ denote the local extreme values of z for each x. When, from the direct visualization, some $\mathcal{W}_i$ looks equal to $\mathcal{W}$, the areas of both cross sections have to match. On the other hand, if it looks that $\mathcal{W}_i \cup \mathcal{W}_j = \mathcal{W}$, then the addition of the area of each cross section have to match the area of $\mathcal{SW}$. As it could happen that $\mathcal{W}_i \cap \mathcal{W}_j \neq \emptyset$, the addition of both areas might not match the area of $\mathcal{SW}$. In this case, given a discretization of each cross section, the area – obtained using either (7),(8) or (9) – of the region conformed by the points that belong to both cross sections has to be subtracted from the addition of the cross sections area of $\mathcal{W}_i, \mathcal{W}_j$. This value has to match the area of $\mathcal{SW}$.

If $\mathcal{W}_i = \mathcal{W}$ for some i, there is only one family of solutions. Besides, the redundant joint is the i-th joint. If, however, $\mathcal{W}_i \cup \mathcal{W}_j = \mathcal{W}$ for some $i \neq j$, then there are two families of solutions: one with the i-th joint as the redundant joint and the other with the j-th. Therefore, they are two one-parameter families of solutions.

Finally, for the case $m > 1$ degrees of redundancy, the procedure for obtaining the 2^m m-parameter families of solutions is the following:

- First, one or two joint are selected as redundant through the workspace analysis explained before.
- The process is repeated for both $\mathcal{W}_i$ and $\mathcal{W}_j$, obtaining one or two new redundant joints for each new workspace. There are up to four sets of two redundant joints each one of them leading to a two-parameter family of solutions.
- Again, the process is repeated in the same way until each set of redundant joints have m joints. There are up to 2^m of these sets and each one of them leads to a m-parameter family of solutions.

3.3. Closed-Form Solution for the IK

Once the redundant joints have been identified and parametrized, a non-redundant reduced manipulator is achieved. If m denotes the number of degrees

of redundancy, a maximum of 2^m sets of m redundant joints can be obtained and, therefore, there exists a partition of $\mathcal{W}$ in a maximum of 2^m parts where each one of them has associated one of these 2^m sets of redundant joints. Denote the elements of such partition by $\overline{\mathcal{W}_1}, \ldots, \overline{\mathcal{W}_{2^m}}$. For every given pose $T \in \mathcal{W}$ there exists $1 \leq i \leq 2^m$ such that $T \in \overline{\mathcal{W}_i}$. Thus, the non-redundant reduced manipulator is the one obtained after parametrizing the joints of the i-th set. Therefore, this criterion allows to decide which solution family should be used for any given pose T. Now, several closed-form methods can be applied attending to the different classes of robots. For manipulators with three consecutive joints whose axes are either parallel or intersect at a single point, Pieper method [5] works properly. For the rest of manipulators, different approaches can be followed: Paul method [6] is the most formal and generic one. It consists of the manipulation of a set of equations obtained from the coefficients of the following set of matrix identities

$$\left(A_{i-1}^{i-2}\right)^{-1} \cdots \left(A_1^0\right)^{-1} T_n^0 = A_i^{i-1} \cdots A_n^{n-1} \tag{10}$$

for $i = 2, \ldots, n$. Here, A_i^{i-1} denotes the homogeneous matrix that relates the frames attached to joints $i-1$ and i, while T_n^0 denotes the end-effector pose matrix. The objective is to isolate the joint variables in some of the equations in order to solve them. Its only drawback is the huge number of combinations required for obtaining a solution. Besides, there exists no guarantee that Paul method can solve the inverse kinematics for all manipulators. For un-resoluble manipulators, different geometric approaches have been developed in literature. One interesting technique, based on the works presented in [54, 55, 56, 57, 58, 59], considers a variation of the original manipulator with three joint axes intersecting at a single point. Then, Pieper closed-form method can be employed for solving the inverse kinematics of that modified manipulator. The solution for the original manipulator is obtained numerically using as initial condition one of the closed-form solutions. Rather than a numerical method, a geometric procedure might be designed for obtaining a closed-form solution based on the obtained one.

The instances for the parametrized joint variables depend on the imposed constraints. From avoiding obstacles, singularities or joint limits to obtaining the most efficient solution in terms of velocity or energy, the different constraints are usually modeling with cost functions trough an optimization process. In particular, given the kinematic relation $\boldsymbol{x} = f(\boldsymbol{q})$ where $\boldsymbol{x}$ denotes the target pose expressed in the operational space X, the optimization can be defined as:

$$\left.\begin{array}{ll} \underset{\boldsymbol{q}}{\text{maximize}} & g(\boldsymbol{q}) \\ \text{subject to} & f(\boldsymbol{q}) = \boldsymbol{x} \end{array}\right\} \tag{11}$$

More precisely, since only the redundant joints acts as variables in the optimiza-

tion process, (11) turns to:

$$\left.\begin{array}{ll} \underset{\boldsymbol{q}_0}{\text{maximize}} & g(\boldsymbol{q}_0) \\ \text{subject to} & f(\boldsymbol{q}) = \boldsymbol{x} \end{array}\right\} \tag{12}$$

where $\boldsymbol{q}_0 = (q_{01}, \ldots, q_{0m})$ is the vector of redundant joint variables.

Examples of cost functions $g(\boldsymbol{q})$ are [3]:

- For avoiding singularities:

$$g(\boldsymbol{q}) = \sqrt{\det(J_G(\boldsymbol{q}) J_G^T(\boldsymbol{q}))}$$

- For avoiding joint limits:

$$g(\boldsymbol{q}) = -\frac{1}{2n} \sum_{i=1}^{n} \left(\frac{q_i - \overline{q_i}}{q_{iM} - q_{im}} \right)$$

  where q_{iM} (q_{im}) denotes the maximum (minimum) joint limit and $\overline{q}_i$ the middle value of the joint range.

- For avoiding obstacles:

$$g(\boldsymbol{q}) = \|\boldsymbol{p}(\boldsymbol{q}) - \boldsymbol{o}\|$$

  where $\boldsymbol{p}(\boldsymbol{q})$ denotes the position vector of the end-effector and $\boldsymbol{o}$ is a suitable point on the obstacle.

4. Examples

To show the advantages of the proposed method, two examples are developed in this section. One of them is a 7 DOF manipulator while the other is a 8 DOF manipulator. Besides, the second example contains a prismatic joint at the beginning of the kinematic chain. Both have a single one-parameter family of solutions. The different computations have been carried out using MATLAB R2015a.

4.1. Kuka LWR 4+

Kuka LWR 4+ is an anthropomorphic arm with seven degrees of freedom (figure 2) and, as a consequence, it has just one degree of redundancy. To identify the redundant joint, the joints meeting the criteria 3.1 are discarded as candidates. For Kuka LWR 4+, the last three joints conform a spherical wrist. Therefore, these joints are discarded. The application of theorem 2.1 through Algorithm 1 gives that the fourth joint leaves a globally degenerated subchain if it is fixed. Then, it cannot be the redundant joint and, therefore, the candidates are the first, the second and the third joint.

For these joints the workspace analysis presented in the preceding section is performed. Without loss of generality, the fixed values assigned to the joint

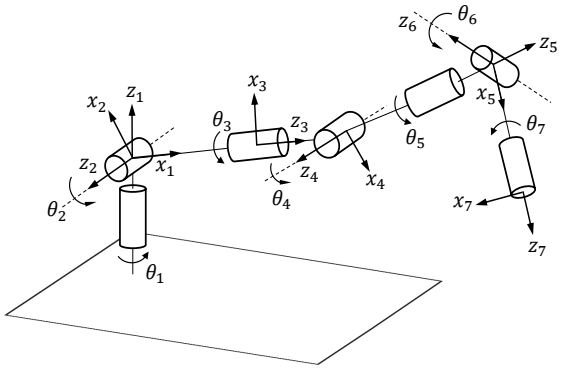

Figure 2: Schematic representation of Kuka LWR 4+

variables are zero. A discretization of the workspace volume for each subchain is generated using Algorithm 2. The volume of the Kuka LWR 4+ is depicted in figure 3a while the rest (figures 3b, 3c and 3d) show the workspace volume of each subchain. From direct visualization it is evident that the workspace shape of the subchain resulting from fixing the third joint ($\mathcal{W}_3$) coincides with the Kuka LWR 4+ whole workspace ($\mathcal{W}$). As $\mathcal{W}$ and $\mathcal{W}_3$ are symmetric with respect to $\boldsymbol{z}_1$, the $\boldsymbol{x}$-$\boldsymbol{z}$ cross section of both workspaces made by setting $q_1 = 0$ can be compared. The area of each cross section is obtained through (9): 0.3101 m^2 for $\mathcal{W}$ and 0.3100 m^2 for $\mathcal{W}_3$. Although the discretization affects the accuracy of the area computation, the results are obviously the same. This confirms that the workspace remains invariant if the third joint is fixed. Therefore, the redundant joint for the Kuka LWR 4+ is the third one.

Once the redundant joint has been selected, and since the Kuka LWR 4+ possesses spherical wrist, Paul closed-form method can be applied for deriving the analytical expressions of each q_i in terms of the pose matrix coefficients. Given:

$$T = \begin{pmatrix} n_x & o_x & a_x & p_x \\ n_y & o_y & a_y & p_y \\ n_z & o_z & a_z & p_z \\ 0 & 0 & 0 & 1 \end{pmatrix},$$

the resolution can be split in two different problems: the position problem, in which from $\mathbf{p} = (p_x, p_y, p_z)$ it is possible to obtain q_1, q_2 and q_4 and the orientation problem, in which from

$$R = \begin{pmatrix} n_x & o_x & a_x \\ n_y & o_y & a_y \\ n_z & o_z & a_z \\ 0 & 0 & 0 \end{pmatrix}$$

q_5, q_6 and q_7 are obtained.

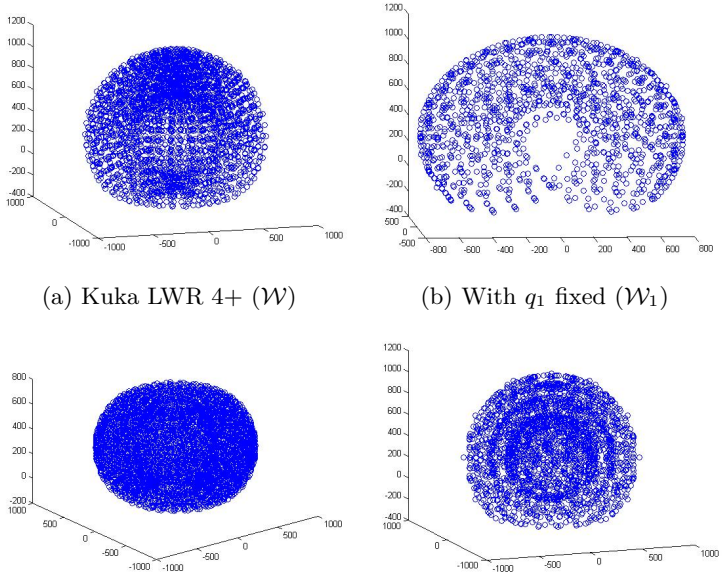

(a) Kuka LWR 4+ ($\mathcal{W}$) (b) With q_1 fixed ($\mathcal{W}_1$)

(c) With q_2 fixed ($\mathcal{W}_2$) (d) With q_3 fixed ($\mathcal{W}_3$)

Figure 3: Kuka LWR 4+ worksapce

For the position problem, (10) is used for obtaining the following identity:

$$\left(A_1^0\right)^{-1} T_7^0 = A_2 \cdots A_7.$$

Now, the fourth column of each matrix is taken:

$$\begin{cases} p_x c_1 + p_y s_1 = c_2(400 + 390c_4) + 390 s_2 c_3 s_4 \\ -p_x s_1 + p_y c_1 = 390 s_3 s_4 \\ p_z - 310 = -390 c_2 c_3 s_4 + s_2(390 c_4 + 400) \end{cases} \tag{13}$$

where, from now on, $c_i = \cos(q_i)$ and $s_i = \sin(q_i)$. Squaring and adding each component gives:

$$p_x^2 + p_y^2 + (p_z - 310)^2 = 400^2 + 390^2 + 2 \cdot 400 \cdot 390 c_4$$

$$\Downarrow$$

$$c_4 = \frac{p_x^2 + p_y^2 + (p_z - 310)^2 - 312100}{312000}$$

Therefore, through the prototype equation (A.2) of Appendix A, the analytical expression for q_4 is derived:

$$q_4 = \text{atan2}(\pm\sqrt{1 - a^2}, a)$$

where atan2$(\cdot,\cdot)$ is the quadrant corrected inverse tangent function and

$$a = \left(\frac{p_x^2 + p_y^2 + (p_z - 310)^2 - 312100}{312000}\right).$$

Once the expression for q_4 is known, the expression for q_1 can be deduced from the following identity:

$$-p_x s_1 + p_y c_1 = 390 s_3 s_4$$

$$\Downarrow$$

$$q_1 = \text{atan2}\left(390 s_3 s_4, \pm\sqrt{p_x^2 + p_y^2 - 390^2 s_3^2 s_4^2}\right) - \text{atan2}(p_y, p_x)$$

through the prototype equation (A.5). Now, the expression for q_2 can be obtained from the following identity using again the prototype equation (A.5):

$$p_z - 310 = -390 c_2 c_3 s_4 + s_2(390 c_4 + 400)$$

$$\Downarrow$$

$$q_2 = \text{atan2}\left(c, \pm\sqrt{a^2 + b^2 - c^2}\right) - \text{atan2}(a, b)$$

with:

$$a = (390 c_4 + 400)$$
$$b = -390 c_3 s_4$$
$$c = p_z - 310$$

Once the position problem has been solved, it is possible to solve the orientation problem. If R_i denotes the matrix that defines the relative orientation of A_i^{i-1}, then:

$$R_1 \cdot R_2 \cdots R_7 = R$$

And, therefore,

$$R_5 \cdot R_6 \cdot R_7 = \underbrace{R_4^{-1} \cdot R_3^{-1} \cdot R_2^{-1} \cdot R_1^{-1} \cdot R}_{\text{Numerical matrix } M}$$

or, analogously:

$$\begin{pmatrix} c_5 c_6 c_7 - s_5 s_7 & -c_7 s_5 - c_5 c_6 s_7 & -c_5 s_6 \\ c_7 s_6 & -s_6 s_7 & c_6 \\ -c_5 s_7 - c_6 c_7 s_5 & c_6 s_5 s_7 - c_5 c_7 & s_5 s_6 \end{pmatrix} = \begin{pmatrix} m_{11} & m_{12} & m_{13} \\ m_{21} & m_{22} & m_{23} \\ m_{31} & m_{32} & m_{33} \end{pmatrix}$$

From M, using the prototype equations (A.2) and (A.3), the following expressions can be obtained:

$$q_6 = \text{atan2}(\pm\sqrt{m_{13}^2 + m_{33}^2}, m_{23})$$
$$q_5 = \text{atan2}(m_{33}/\sin(q_6), -m_{13}/\sin(q_6))$$
$$q_7 = \text{atan2}(-m_{22}/\sin(q_6), m_{21}/\sin(q_6))$$

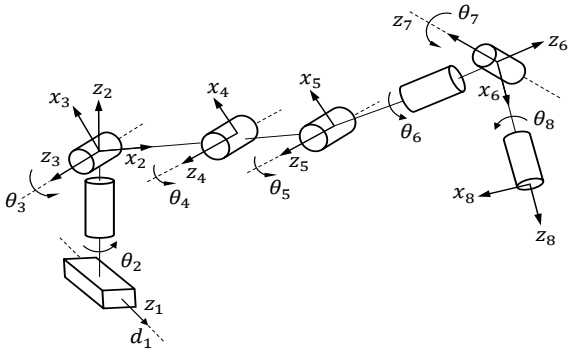

Figure 4: Schematic representation of Stäubli TX90 mounted on a translational motion unit

4.2. Extended Stäubli TX90 mounted on a translational motion unit

Stäubli TX90 is an industrial manipulator with six degrees of freedom and spherical wrist. This manipulator has been mounted on a linear track, that can be seen as an additional prismatic joint. Besides, it has been extended by adding an extra revolute joint whose axis is parallel to the axes of the third and fourth joints (figure 4). As in the precedent example, the three last joints are discarded for being the redundant ones since they conform a spherical wrist. Once the first joint – the prismatic one – is fixed, for testing if any other joint should be discarded according to the list 3.1, Algorithm 1 is applied in order to find out the globally degenerated reduced manipulators. From the seven different kinematic subchains, the one obtained after fixing the second joint – the first revolute joint – is a globally degenerated subchain. Therefore, the third, the fourth and the fifth joints are candidates for being redundant.

For these joints the workspace analysis is performed using Algorithm 2. The prismatic joint variable is set as zero (its motion lies within the range $[0, 2]$). The extended Stäubli TX90 workspace is depicted in figure 5a while the workspaces of the subchains are depicted in figures 5b, 5c and 5d. In this case, as in the precedent example, there exists i such that $\mathcal{W}_i = \mathcal{W}$. It is clear, from direct visualization, that $\mathcal{W}_5 = \mathcal{W}$. Furthermore, the workspaces dimensions also show that $\mathcal{W}_5 = \mathcal{W}$. Indeed, the dimensions of $\mathcal{W}$ are $3m \times 4m \times 3m$, while the dimensions fo the workspaces after the parametrization of the candidates are:

- $\mathcal{W}_3$: $1.8m \times 2m \times 2m$ (figure 5b).
- $\mathcal{W}_4$: $2m \times 2m \times 2m$ (figure 5c).
- $\mathcal{W}_5$: $3m \times 3m \times 4m$ (figure 5d).

Again, setting $q_2 = 0$ returns the $\boldsymbol{x}$-$\boldsymbol{z}$ cross section. Moreover, if (9) is used for calculating the cross section areas of $\mathcal{W}$ and $\mathcal{W}_5$, the resulting value is the same (up to some discretization error) is the same:

$$A_{\mathcal{W}} = 2.560m^2 \quad A_{\mathcal{W}_5} = 2.555m^2$$

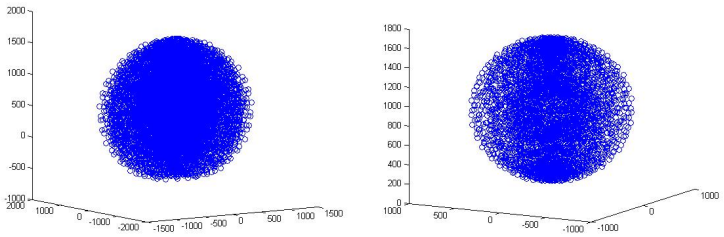

(a) Extended Stäubli TX90 ($\mathcal{W}$) (b) With q_3 fixed ($\mathcal{W}_3$)

(c) With q_4 fixed ($\mathcal{W}_4$) (d) With q_5 fixed ($\mathcal{W}_5$)

Figure 5: Extended Stäubli TX90 workspace

This confirms that the redundant joint for the extended Stäubli TX90 is the fifth one from which it can be obtained the one-parameter family of solutions.

As in the case of the Kuka LWR 4+, the presence of spherical wrist allows to use Paul method for obtaining the closed-form solutions. The decomposition into the position and orientation problems can be made. For this example, q_5 will work as the parameter of the family of solutions.

For the position problem, a geometric method can be used to calculate d_1. The position vector $\mathbf{p}$ is projected onto the $\boldsymbol{x}$-$\boldsymbol{y}$ plane. If the projection is denoted $\pi(\mathbf{p})$, then d_1 is obtained so $d_1 = \min\{\|d_1 - \pi(\mathbf{p})\|\}$. For the remaining joint variables, the following identity is used:

$$\left(A_2^0\right)^{-1} T_8^0 = A_3 \cdots A_8 \tag{14}$$

The position vector from both sides of (14) is:

$$p_x c_2 + p_y s_2 = 425 s_3 + 300 c_{34} + 425 c_{345} + 50 \tag{15}$$

$$p_y c_2 - p_x s_2 = 50 \tag{16}$$

$$p_z - 478 = 425 c_3 + 300 s_{34} + 425 s_{345} \tag{17}$$

Equation (16):

$$-p_x s_2 + p_y c_2 = 50$$

can be solved using the prototype equation (A.5) of Appendix A. Thus, the analytical expression for q_2 is:

$$q_2 = \text{atan2}\left(50, \pm\sqrt{p_x^2 + p_y^2 - 50^2}\right) - \text{atan2}(p_y, p_x)$$

Now, equations (15) and (17) are squared and added. Once the terms have been regrouped, the expression obtained is:

$$\alpha = 451250 - 255000s_4 - 361250s_{45} + 255000c_5 \tag{18}$$

where $\alpha = (p_x c_2 + p_y s_2 - 50)^2 + (p_z - 478)^2$.

As q_5 is the redundant joint and it is parametrized at some value, (18) is simplified to:

$$451250 + 255000c_5 - \alpha = (255000 + 361250c_5)s_4 + 361250s_5 c_4$$

Using the prototype equation (A.5) of Appendix A, the analytical expression for q_4 is:

$$q_4 = \text{atan2}\left(c, \pm\sqrt{a^2 + b^2 - c^2}\right) - \text{atan2}(a, b),$$

with:

$$\begin{aligned} a &= 361250s_5 \\ b &= (255000 + 361250c_5) \\ c &= 451250 + 255000c_5 - \alpha \end{aligned}$$

Finally, as the expression for q_4 is known and q_5 is parametrized at some value, (17) is equivalent to:

$$p_z - 478 = (300 + 300s_4 + 425s_{45})c_3 + (300c_4 + 425c_{45})s_3$$

which can be solve using again the prototype equation (A.5):

$$q_3 = \text{atan2}\left(c, \pm\sqrt{a^2 + b^2 - c^2}\right) - \text{atan2}(a, b),$$

with:

$$\begin{aligned} a &= 300 + 300s_4 + 425s_{45} \\ b &= 300c_4 + 425c_{45} \\ c &= p_z - 478 \end{aligned}$$

The orientation problem is solved analogously as in the case of the Kuka LWR 4+.

5. Conclusions

This work proposes a novel method to derive closed-form solutions for the inverse kinematic problem of redundant serial manipulators. Unlike other methods found in literature, the method exposed in this work allows an efficient selection of *redundant joints*, whose joint variables can be parametrized or fixed

at an arbitrary value. First, an upper bound for the number of different closed-form solutions for a particular pose of the manipulator is given. If m denotes the number of degrees of redundancy there are up to 2^m families of closed-form solutions. The selection of the sets of redundant joints that gives those closed-form solutions is made based on the discarding criteria 3.1 and the workspace analysis introduced in section 3.2. Once the redundant joints have been identified, the inverse kinematics of the reduced non-redundant manipulator can be solved using Pieper, Paul or particular geometric methods. As closed-form methods are used for non-redundant reduced manipulators, the procedure proposed in this work has clear advantages over the numerical methods designed for redundant manipulators. Besides, in comparison with other closed-form methods, the simplicity of this strategy makes it suitable for general redundant manipulators. In fact, for any given manipulator with three consecutive joints whose axes are either parallel or intersects at a single point, the inverse kinematics problem is completely solved analytically using Pieper's theorem.

Acknowledgement

This work has been partially supported by the Spanish CICYT projects DPI2013-40882-P, DPI2016-80077R and by the Spanish predoctoral grant BES-2012-059884.

Appendix A. Prototype Trigonometric Equations

The following list shows the main prototype trigonometric equations used in this paper. A more complete list of such kind of equations can be found in [6, 60]:

$$\sin(\theta) = a \Longrightarrow \theta = \text{atan2}\left(a, \pm\sqrt{1-a^2}\right) \tag{A.1}$$

$$\cos(\theta) = a \Longrightarrow \theta = \text{atan2}\left(\pm\sqrt{1-a^2}, a\right) \tag{A.2}$$

$$\left.\begin{array}{l}\sin(\theta) = a \\ \cos(\theta) = b\end{array}\right\} \Longrightarrow \theta = \text{atan2}(a, b) \tag{A.3}$$

$$a\cos(\theta) + b\sin(\theta) = 0 \Longrightarrow \left\{\begin{array}{l}\theta = \text{atan2}(-a, b) \\ \text{or} \\ \theta = \text{atan2}(a, -b)\end{array}\right. \tag{A.4}$$

$$\begin{array}{c} a\cos(\theta) + b\sin(\theta) = c \Longrightarrow \theta = \text{atan2}(c, \pm\alpha) - \text{atan2}(a, b) \\ \text{where } \alpha = \sqrt{a^2 + b^2 - c^2}\end{array} \tag{A.5}$$

$$\left.\begin{array}{l}a\cos(\theta_1) + b\cos(\theta_2) = e \\ a\sin(\theta_1) + b\sin(\theta_2) = f\end{array}\right\} \Longrightarrow \theta_1 = \text{atan2}\left(\beta, \pm\sqrt{e^2 + f^2 - \beta^2}\right) \quad \text{where } \beta = \frac{a^2 + e^2 + f^2 - b^2}{2a} \tag{A.6}$$

References

[1] J. Craig, Introduction to Robotics: Mechanics and Control, Addison-Wesley Longman Publishing Company, 1989.

[2] J. Denavit, R. S. Hartenberg, A kinematic notation for lower-pair mechanisms based on matrices, Journal of Applied Mechanics 22 (2) (1965) 215 – 221.

[3] B. Siciliano, L. Sciavicco, L. Villani, G. Oriolo, Robotics: Modelling, Planning and Control, Springer Publishing Company, 2008.

[4] M. Spong, S. Hutchinson, M. Vidyasagar, Robot Modeling and Control, John Wiley and Sons, 2006.

[5] D. Pieper, The kinematics of manipulation under computer control, Ph.D. thesis, Stanford Artificial Intelligence Laboratory – Stanford University (1968).

[6] R. Paul, Robot Manipulators: Mathematics, Programming and Control, The MIT Press, 1981.

[7] P. Chang, A closed-form solution for inverse kinematics of robot manipulators with redundancy, IEEE Journal on Robotics and Automation 3 (5) (1987) 393 – 403.

[8] O. Ivlev, A. Gräser, An analytical method for the inverse kinematics of redundant robots, in: International Conference Advanced Robotics, Intelligent Automation and Active Systems, Bremen, Germany, 1997, pp. 416 – 421.

[9] O. Ivlev, A. Gräser, Resolving redundancyof series kinematic chains through imaginary links, in: International Conference on Computational Engineering in Systems Applications (CESA98), Nabeul- Hammamet, Tunisia, 1998, pp. 477 – 482.

[10] D. Jung, Y. Yoo, J. Koo, M. Song, S. Won, A novel redundancy resolution method to avoid joint limits and obstacles on anthropomorphic manipulator, in: Society of Instrument and Control Engineers (SICE) Annual Conference, Tokyo, Japan, 2011, pp. 924 – 929.

[11] M. Shimizu, H. Kakuya, W. Yoon, K. Kitagaki, K. Kosuge, Analytical inverse kinematic computation for 7-DoF redundant manipulator with joint limits and its application to redundancy resolution, IEEE Transactions on Robotics 24 (5) (2008) 1131 – 1142.

[12] C. Yu, M. Jin, H. Liu, An analytical solution for inverse kinematic of 7-DOF redundant manipulators with offset-wrist, in: IEEE International Conference on Mechatronics and Automation, Chengdu, China, 2012, pp. 92 – 97.

[13] L. Huang, R. Jiang, A new method of inverse kinematics solution for industrial 7DoF robot, in: 32nd Chinese Control Conference (CCC), Xi'an, China, 2013, pp. 6063 – 6065.

[14] Y. Liu, D. Wang, J. Sun, L. Chang, C. Ma, Y. Ge, L. Gao, Geometric approach for inverse kinematics analysis of 6-DOF serial robot, in: IEEE International Conference on Information and Automation, Lijiang, China, 2015, pp. 852 – 855.

[15] G. Singh, J. Claassens, An analytical solution for the inverse kinematics of a redundant 7DoF manipulator with link offsets, in: IEEE/RSJ International Conference on Intelligent Robots and Systems (IROS), Taipei, Taiwan, 2010, pp. 2976 – 2982.

[16] Y. Wei, S. Jian, S. He, Z. Wang, General approach for inverse kinematics of nR robots, Mechanism and Machine Theory 75 (2014) 97 – 106.

[17] J. Baillieul, Avoiding obstacles and resolving kinematic redundancy, in: IEEE International Conference on Robotics and Automation (ICRA), San Francisco, CA, USA, 1986, pp. 1698 – 1704.

[18] S. Buss, Introduction to inverse kinematics with Jacobian transpose, pseudoinverse and Damped Least Squares methods., Tech. rep., University of California, San Diego (2009).

[19] S. Buss, J. Kim, Selectively Damped Least Squares for inverse kinematics., Journal of Graphics Tools 10 (3) (2005) 37 – 49.

[20] A. De Luca, G. Oriolo, The reduced gradient method for solving redundancy in robot arms, RoboterSysteme 7 (1991) 117 – 122.

[21] P. Hsu, J. Hauser, S. Sastry, Dynamic control of redundant manipulators, in: American Control Conference, Atlanta, GA, USA, 1988, pp. 2135 – 2139.

[22] H. Lau, L. Wai, A Jacobian-based redundant control strategy for 7DOF WAM, in: Proceedings of the Conference on Control, Automation, Robotics and Vision (ICARV), Singapore, 2002, pp. 1060 – 1065.

[23] D. Nenchev, Redundancy resolution through local optimization: A review, Journal of Robotics Systems 6 (6) (1989) 769 – 798.

[24] C. Pozna, E. Horváth, J. Hollósi, The inverse kinematics problem, a heuristical approach, in: IEEE International Symposium on Applied Machine Intelligence and Informatics (SAMI), Herlany, Slovakia, 2016, pp. 299 – 304.

[25] R. Sánchez-Alonso, J. González-Barbosa, E. Castillo-Castañeda, M. García-Murillo, Kinematic analysis of a novel reconfigurable parallel robot, Revista Iberoamericana de Automática e Informática Industrial (RIAI) 13 (2) (2016) 247 – 257.

[26] Y. Sung, D. Cho, M. Chung, A constrained optimization approach to resolving manipulator redundancy, Journal of Robotics Systems 13 (5) (1996) 275 – 288.

[27] W. Wang, Y. Suga, H. Iwata, S. Sugano, Solve inverse kinematics through a new quadratic minimization technique, in: IEEE/ASME International Conference on Advanced Intelligent Mechatronics (AIM), Kachsiung, Taiwan, 2012, pp. 306 – 313.

[28] C. Wampler, Manipulator inverse kinematic solutions based on vector formulations and damped least-squares methods, IEEE Transactions on Systems, Man, and Cybernetics 16 (1) (1986) 93 – 101.

[29] A. Fratu, L. Vermeiren, A. Dequidt, Using the redundant inverse kinematics system for collision avoidance, in: International Symposium on Electrical and Electronics Engineering (ISEEE), Galati, Romania, 2010, pp. 88 – 93.

[30] J. S. Kim, J. H. Jeong, J. H. Park, Inverse kinematics and geometric singularity analysis of a 3-SPS/S redundant motion mechanism using conformal geometric algebra, Mechanism and Machine Theory 90 (2015) 23 – 36.

[31] J. S. Kim, J. H. Jeong, J. H. Park, Inverse kinematics of a redundant manipulator based on conformal geometry using geometric approach, in: 12th International Conference on Informatics in Control, Automation and Robotics (ICINCO), Colmar, France, 2015, pp. 179 – 185.

[32] D. Drexler, Solution of the closed-loop inverse kinematics algorithm using the Crank-Nicolson method, in: IEEE International Symposium on Applied Machine Intelligence and Informatics (SAMI), Herlany, Slovakia, 2016, pp. 351 – 356.

[33] N. Vahrenkamp, D. Muth, P. Kaiser, T. Asfour, IK-Map: An enhanced workspace representation to support inverse kinematics solvers, in: IEEE-RAS International Conference on Humanoid Robots (Humanoids), Seoul, South Korea, 2015, pp. 785 – 790.

[34] J. Hollerbach, Optimum kinematic design for a seven degree of freedom manipulator, in: Robotics Research: The Second International Symposium, Yyoto, Japan, MIT Press, 1985, pp. 215 – 222.

[35] R. Judd, R. Van Til, A perfomance measure for computing the reverse kinematic solution for robots with redundant degrees of freedom, in: International Conference on Decision and Control, Fort Lauderdale, FL, USA, 1985, pp. 360 – 361.

[36] K. Tokarz, S. Kieltyka, Geometric approach to inverse kinematics for arm manipulator, in: WSEAS International Conference on Systems: Part of the 14th WSEAS CSCC Multiconference - Volume II, Corfu Island, Greece, 2010, pp. 682 – 687.

[37] A. Hemami, A more general closed-form solution to the inverse kineamatics of mechanical arms, Advanced Robotics of the Robotics Society of Japan 2 (4) (1988) 315 – 325.

[38] H. Schrake, H. Rieseler, F. Wahl, Symbolic kinematics inversion of redundant robots, in: International Symposium on Foundations of Robotics, Berlin, Germany, 1990, pp. 1 – 10.

[39] H. Schrake, H. Rieseler, F. Wahl, Manipulator classification by means of a kinematics description language, in: International Conference on Advanced Robotics (ICAR), Pisa, Italy, 1991, pp. 678 – 682.

[40] H. Heiss, Die explizite lösung der kinematischen gleichung für eine klasse von industrierrobotern, Ph.D. thesis, Technische Universität München (TUM) (1985).

[41] S. Lee, A. Bejczy, Redundant arm kinematic control based on parametrization, in: IEEE International Conference on Robotics and Automation, Sacramento, CA, USA, 1991, pp. 458 – 465.

[42] R. Podhorodeski, A. Goldenberg, R. Fenton, Resolving redundant manipulator joint rates and indentifying special arm configurations using Jacobian null-space bases, IEEE Transactions on Robotics and Automation 7 (5) (1991) 607 – 618.

[43] R. Diankov, Automated construction of robotics manipulation programs, Ph.D. thesis, Robotics Institute, Carnegie Mellon University (2010).

[44] H. Heiss, Redundancy resolution for an eight-axis manipulator, in: Computational Kinematics, Scholss Dagstuhl, Germany, Springer Netherlands, 1993, pp. 55 – 66.

[45] M. Kauschke, Closed form solutions applied to redundant serial link manipulators, Mathematics and Computers in Simulation 41 (5) (1996) 509 – 516.

[46] R. Tatum, D. Lucas, J. Weaver, J. Perkins, Geometrically motivated inverse kinematics for an arm with 7 degrees of freedom, in: MTS/IEEE OCEANS, Washington DC, USA, 2015, pp. 1 – 6.

[47] M. Qingmei, W. Pengcheng, D. Jiaming, S. Huiping, L. Minzhou, An algorithm of inverse kinematics for manipulator with redundancy, in: IEEE International Conference on Cyber Technology in Automation, Control, and Intelligent Systems (CYBER), Shenyang, China, 2015, pp. 54 – 58.

[48] H. Dong, Z. Du, G. Chirikjian, Workspace density and inverse kinematics for planar serial revolute manipulators, Mechanism and Machine Theory 70 (2013) 508 – 522.

[49] K. Gupta, B. Roth, Design considerations for manipulator workspace, ASME. Journal of Mechanical Design 104 (4) (1982) 704 – 711.

[50] T. Lee, D. Yang, On the evaluation of manipulator workspace, ASME Journal of Mechanisms, Transmissions, and Automation in Design 105 (1) (1983) 70 – 77.

[51] D. Yang, T. Lee, On the workspace of mechanical manipulators, ASME Journal of Mechanisms, Transmissions, and Automation in Design 105 (1) (1983) 62 – 69.

[52] K. Abdel-Malek, S. Othman, Multiple sweeping using the Denavit-Hartenberg representation method, Computer-Aided Design 31 (9) (1999) 567 – 583.

[53] K. Abdel-Malek, H. Yeh, N. Khairallah, Workspace, void, and volume determination of the general 5DOF manipulator, Mechanics of Structures and Machines 27 (1) (1999) 89 – 115.

[54] H. Ananthanarayanan, R. Ordóñez, Real-time Inverse Kinematics of $(2n+1)$-DOF hyper-redundant manipulator arm via a combined numerical and analytical approach, Mechanism and Machine Theory 91 (2015) 209 – 226.

[55] S. Kucuck, Z. Bingul, The inverse kinematics solutions of fundamental robot manipulators with offset wrist, in: IEEE International Conference on Mechatronics (ICM), Taipei, Taiwan, 2005, pp. 197 – 202.

[56] S. Kucuk, Z. Bingul, Inverse kinematics solutions for industrial robot manipulators with offset wrists, Applied Mathematical Modelling 38 (7) (2014) 1983 – 1999.

[57] H. Pan, B. Fu, L. Chen, J. Feng, The inverse kinematics solutions of robot manipulators with offset wrist using the offset modification method, in: Selected Papers from the International Conference on Automation and Robotics (ICAR 2011): Advances in Automation and Robotics, Vol.1, Springer Berlin Heidelberg, 2012, pp. 655 – 663.

[58] M. Wu, Y. S. Kung, F. C. Lee, W. C. Chen, Inverse kinematics of robot manipulators with offset wrist, in: International Conference on Advanced Robotics and Intelligent Systems (ARIS), Taipei, Taiwan, 2015, pp. 1 – 6.

[59] I. Zaplana, J. Claret, L. Basanez, Kinematic analysis of redundant robotic manipulators: application to Kuka LWR 4+ and ABB Yumi, Revista Iberoamericana de Automática e Informática Industrial In Press.

[60] H. Rieseler, H. Schrake, F. Wahl, Symbolic computation of closed form solutions with prototype equations, in: International Workshop on Advances in Robot Kinematics, Linz, Austria, 1990, pp. 343 – 351.